5-21-2021

Control-Oriented Nonlinear Modeling of Polyvinyl Chloride (Pvc) Gel Actuators

Mohammed Al-Rubaiai
Michigan State University

Xinda Qi
Michigan State University

Zachary Frank
University of Nevada, Las Vegas

Ryohei Tsuruta
Toyota Motor Engineering and Manufacturing North America

Umesh Gandhi
Toyota Motor Engineering and Manufacturing North America

See next page for additional authors

Repository Citation

Al-Rubaiai, M., Qi, X., Frank, Z., Tsuruta, R., Gandhi, U., Kim, K. J., Tan, X. (2021). Control-Oriented Nonlinear Modeling of Polyvinyl Chloride (Pvc) Gel Actuators. *IFAC-PapersOnLine, 54*(20), 304-309. Amsterdam, Netherlands: Elsevier; International Federation of Automatic Control (IFAC).
http://dx.doi.org/10.1016/j.ifacol.2021.11.191

Authors

Mohammed Al-Rubaiai, Xinda Qi, Zachary Frank, Ryohei Tsuruta, Umesh Gandhi, Kwang J. Kim, and Xiaobo Tan

Available online at www.sciencedirect.com

ScienceDirect

IFAC PapersOnLine 54-20 (2021) 304–309

Control-oriented Nonlinear Modeling of Polyvinyl Chloride (PVC) Gel Actuators

Mohammed Al-Rubaiai * **Xinda Qi** * **Zachary Frank** ** **Ryohei Tsuruta** *** **Umesh Gandhi** *** **Kwang J. Kim** ** **Xiaobo Tan** *

* *Department of Electrical and Computer Engineering, Michigan State University, East Lansing, MI 48824,USA (e-mails: alrubaia@msu.edu (M.A.), qixinda@msu.edu (X.Q.), xbtan@msu.edu (X.T.))*
** *Department of Mechanical Engineering , University of Nevada, Las Vegas, NV 89154,USA (e-mails: zachary.frank@unlv.edu (Z.F.), kwang.kim@unlv.edu (K.K.))*
*** *Toyota Motor North America, Ann Arbor, MI 48105, USA (e-mails: ryohei.tsuruta@toyota.com (R.T.), umesh.gandhi@toyota.com (U.G.))*

Abstract: Polyvinyl chloride (PVC) gel-based actuators are a new class of soft, electroactive polymer actuators with several attractive properties, including low cost, large compliance, large strain output, high-stress output, fast response, and stability against thermal influence. While PVC gel actuators are quickly gaining attention, they remain largely unexplored despite their great potential in a long list of applications compared with many other smart material actuators. In particular, little work has been reported on modeling nonlinear dynamics of PVC actuators. In this work a nonlinear, control-oriented Hammerstein model, with a polynomial nonlinearity preceding a transfer function, is proposed to capture the amplitude-dependent frequency responses of PVC gel actuators. A systematic procedure for identifying the model parameters is developed. The efficacy of the modeling approach is demonstrated with experimental voltage-displacement data collected from a PVC gel actuator prototype, where the model is able to predict the input amplitude-dependent dynamic response.

Keywords: PVC gel actuator, electroactive polymer, Hammerstein model, frequency response, describing function

1. INTRODUCTION

Soft actuators based on smart materials have been widely studied owing to their flexibility, compactness, and great potential in various applications [Choi et al. (2005); Sharif et al. (2018); Li and Hashimoto (2016)]. As one type of electroactive polymers, Polyvinyl chloride (PVC) gel actuators exhibit attractive performance in displacement output, force output, response speed, and behavioral stability, which make them a promising artificial muscle technology [Hwang et al. (2019); Furuse and Hashimoto (2017); Li et al. (2019); Ali et al. (2011)], with application to optical focusing lenses, wearable assistive spats, tactile display, vibrotactile actuator, and micro gripper among others [Hirai et al. (2009); Li et al. (2015); Park et al. (2019, 2017); Hirai et al. (2013)].

With the development of different structures and configurations for PVC gel actuators, underlying actuation mechanisms for PVC gels have been explored. The polarity of the PVC and the plasticizer (typically, dibutyl adipate, or DBA) molecules allows them to rearrange and move under an electric field, generating the electrophoresis current from charge injection [Xia and Hirai (2009)]. The close relationship between the formation of a plasticizer-rich layer and the gel creeping motion around a mesh-structured anode under an electric field is discussed [Ali et al. (2011)]. Based on these assumptions and explorations, several analytical models have been proposed, including a bending deformation model with solvent-rich layer formation theory [Asaka and Hashimoto (2018)], a model for contraction type PVC gel actuator with equivalent circuit analysis [Shibagaki et al. (2010)], a force and deformation model based on Hill's muscle model [Li and Hashimoto (2015)], and an electromechanical model for PVC gel actuator with addition of ionic liquids [Asaka and Hashimoto (2020)]. Moreover, a numerical model has been developed by using the Maxwell stress tensor and nonlinear elastic material models for FEM simulations of the PVC gel actuators [Frank et al. (2019)]. While these models are generally instrumental in predicting static deformation and force output of PVC gel actuators, little work has been reported

⋆ This work was supported in part by Toyota Motor North America and a Michigan State University Strategic Partnership Grant (16-SPG-Full-3236). The authors (ZF and KJK) from UNLV acknowledge partial financial support from the US National Science Foundation (NSF), Partnerships for International Research and Education (PIRE) Program, Grant No. 1545857. Any opinions, findings, and conclusions or recommendations expressed in this material are those of the author(s) and do not necessarily reflect the views of the NSF.

10.1016/j.ifacol.2021.11.191

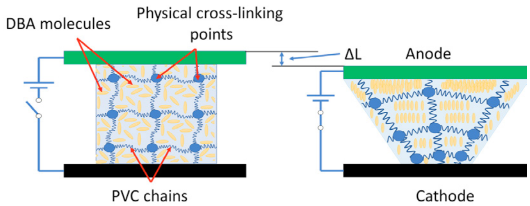

Fig. 1. Schematic diagram of PVC gel internal structure and its change with an applied electric field.

on modeling nonlinear dynamic behavior for these actuators. Such models will be important for effective design of controllers for PVC gel actuators in their versatile applications.

In this paper, we present a data-driven modeling approach to capture the observed nonlinear dynamics of PVC gel actuators, where the voltage input – displacement output frequency response shows pronounced dependence on the input amplitude. A Hammerstein-type model is proposed, where a polynomial nonlinearity precedes a linear system, and the identification procedure for the model is presented. In particular, the linear system is identified based on the empirical frequency response of the actuator at a relatively low input amplitude, and the coefficients of the polynomial nonlinearity are determined via a least squares minimization procedure. The effectiveness of the proposed nonlinear model is supported by its capability to predict the experimentally observed dynamic responses under inputs of different amplitudes.

The remainder of the paper is organized as follows. The process for PVC gel membrane fabrication is first presented in Section 2. The experimental setup is described in Section 3.1, followed by the dynamic modeling approach in Section 3.2. Experimental results are discussed in Section 4. Finally, concluding remarks, including a discussion on future work, are provided in Section 5.

2. PVC GEL MEMBRANE FABRICATION

The PVC gel microstructure was studied by Ali et al. (2011)). The gel contains PVC polymer chains loosely connected via physical crosslinking, with the internal space of the polymer chain matrix being filled with a plasticizer (Fig. 1). When no electric field is applied, the PVC gel dipoles have no preferred orientation; however, under an applied electric field, the plasticizer molecules are polarized and dipole rotation of the PVC chains occurs, pulling the PVC gel toward the anode. PVC gel membranes are cast, with thicknesses ranging from hundreds of micrometers up to several millimeters.

The fabrication process of the electroactive PVC gel is illustrated in Fig. 2 (a). First, PVC powders and DBA plasticizer (Sigma-Aldrich, St. Louis, MO, USA) are poured into the tetrahydrofuran (THF) solvent (Sigma-Aldrich, St. Louis, MO, USA). The solution is stirred for four hours at 50 °C to fully dissolve the PVC and the DBA in the THF solvent. To fabricate a flat, transparent PVC gel membrane, the fully dissolved solution is then poured into a glass petri dish and sits at room temperature for approximately 48 h, until the solvent THF has evaporated.

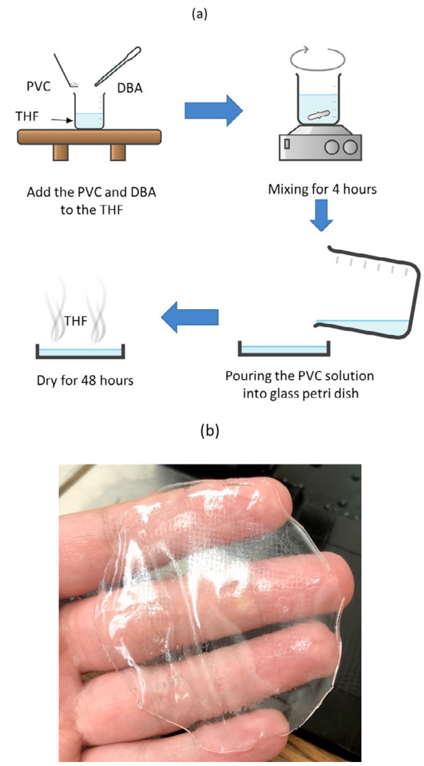

Fig. 2. (a) Process of preparation of PVC gel membrane; (b) A photograph of a fabricated PVC gel membrane.

The fabricated PVC gel membrane is transparent, soft, pliable, and lightweight; see Fig. 2 (b). The weight ratio of PVC to DBA can be adjusted to alter the material characteristics of the membranes, and in this study a weight ratio of 1:8 (PVC to DBA) is used.

3. MODELING APPROACH

This section describes the proposed system identification process used to model the nonlinear dynamics of a contraction-type PVC gel actuator. Firstly, we describe the experimental setup for data collection. We then explain the nonlinear system identification approach using the describing function method [Slotine et al. (1991)].

Table 1. Thicknesses of PVC gel actuator layers.

Layer	Material	Thickness	Units
Anode	stainless steel mesh	432	μm
Membrane	PVC gel	396	μm
Cathode	stainless steel foil	50	μm

3.1 Experimental Setup

The experimental data used in this study is obtained by actuating a PVC gel actuator, where the voltage is the input and the displacement measured is the output. The experimental setup is shown in Fig. 3. The actuator consists of a PVC gel membrane placed between a stainless-steel mesh anode and a cathode made from stainless-steel foil. The thickness of each layer is shown in Table 1. When a DC field is applied, the PVC gel exhibits an anodophilic deformation onto the mesh anode, with the gel moving

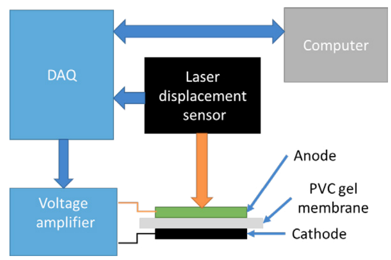

Fig. 3. Experimental setup for characterizing the PVC gel actuator.

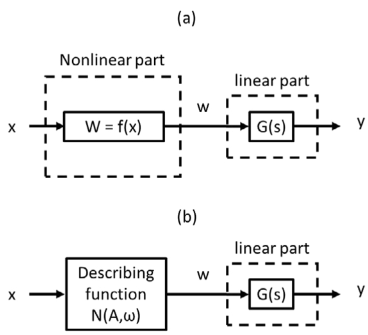

Fig. 4. (a) Proposed Hammerstein model structure for PVC gel actuator dynamics; (b) Use of the describing function of the nonlinear element for system identification.

into the holes in the mesh. This causes a bulk contraction of actuator to occur in the thickness direction. When the DC field is removed, the actuator quickly moves back to its original shape as a result of the gel's elasticity. A laser displacement sensor (OADM20I6441/S14F, Baumer Electric) is mounted above the actuator to measure the displacement. A high voltage amplifier (AMJ-2B20 from Matsusada Precision) is used to drive the actuator. A dSPACE system is used for control signal generation, sensing data acquisition, and processing.

3.2 Dynamic Modeling

The describing function method is considered an extended version of the frequency response method, and it can be used to approximately analyze and predict nonlinear behaviors [Slotine et al. (1991)]. The describing function of a nonlinear system, $N(A, \omega)$, is defined to capture the gain and phase shift between the fundamental harmonic component of the output and a sinusoidal input:

$$N(A, \omega) = \frac{Y}{A} \angle \phi \tag{1}$$

where A and ω represent the amplitude and the angular frequency of the sinusoidal input, respectively, Y denotes the amplitude of the fundamental harmonic component of the output, and ϕ denotes the phase shift of the fundamental harmonic component of the output with respect to the sinusoidal input.

The PVC gel actuator shows dynamic behavior that is dependent on the amplitude of the voltage input (see the measured frequency responses in Fig. 6). In this paper we propose to capture such nonlinear dynamics with a Hammerstein model structure, i.e., a static nonlinearity followed by a linear time-invariant (LTI) system, as illustrated in Fig. 4(a). While there could be a wide range of choices for the nonlinearity $f(x)$, we consider the form of odd polynomials:

$$w = f(x) = \sum_{i=1}^{n} c_i x^{2i-1} \tag{2}$$

for some $n \geq 1$, where c_i, $i = 1, \cdots, n$, are coefficients.

We first illustrate the computation of the describing function $N(A, \omega)$ with an example of $n = 2$, where

$$w = c_1 x + c_2 x^3 \tag{3}$$

Given an input $x(t) = A\sin(\omega t)$, the output $w(t) = c_1 A \sin(\omega t) + c_2 A^3 \sin^3(\omega t)$ can be expanded as a Fourier series, with the fundamental frequency term represented as

$$w_1(t) = a_1 \cos(\omega t) + b_1 \sin(\omega t) \tag{4}$$

Because $f(x)$ is an odd function, one has $a_1 = 0$, and the coefficient b_1 is evaluated as

$$\begin{aligned} b_1 &= \frac{1}{\pi} \int_{-\pi}^{\pi} [c_1 A \sin(\omega t) + c_2 A^3 \sin^3(\omega t)] \sin(\omega t) d(\omega t) \\ &= c_1 A + (\frac{3}{8}) c_2 A^3 \end{aligned} \tag{5}$$

Therefore, we have

$$w_1(t) = \left[c_1 A + (\frac{3}{8}) c_2 A^3 \right] \sin(\omega t) \tag{6}$$

and the describing function as

$$N(A, \omega) = c_1 + (\frac{3}{8}) c_2 A^2 \tag{7}$$

Note that due to the odd nature of this nonlinearity, the describing function is real, with no phase shift between its output and input for any frequency ω.

For the LTI system $G(s)$ in Fig. 4, one can identify it based on the measured frequency response when the input amplitude is relatively small. We now describe how to use $G(s)$, along with the describing function for the nonlinear element (parameterized with c_i, $i = 1, \cdots, n$), to identify c_i based on experimentally measured frequency responses at different input amplitudes.

Let the frequency response of $G(s)$ be denoted as

$$G(j\omega) = M_L(\omega) \angle(\omega) \tag{8}$$

The overall gain for the Hammerstein system in Fig. 4 can be represented as

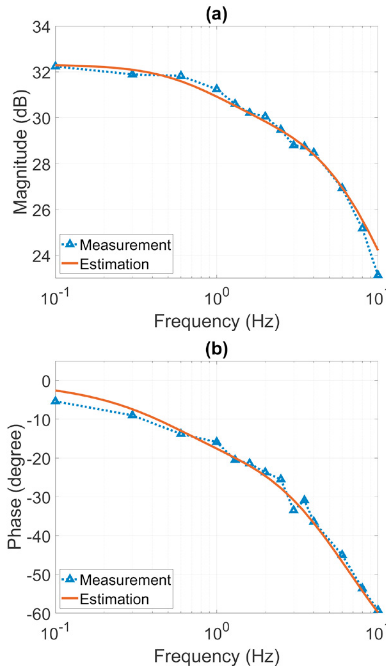

Fig. 5. Measured frequency response of the PVC gel actuator for the amplitude of 300 V, and the frequency response of the identified linear model: (a) Magnitude plot; (b) phase plot.

$$M_s(A,\omega) = N(A,\omega)M_L(\omega) = \sum_{i=1}^{N} c_i h_i(A,\omega) \quad (9)$$

where $h_i(A,\omega)$, $i = 1,\cdots,n$, represent the describing function terms associated with c_i. For example, when $n = 2$, from Eq. (7), $h_1 = 1$, $h_2 = \frac{3}{8}A^2$.

Now suppose that there are N ($N \geq n$) measurements of the overall system gain, $\{d_k(A_k,\omega_k)\}_{k=1}^{N}$, collected under different combinations of input frequencies ω_k and amplitudes A_k. We can then aim to find the set of coefficients $\{c_i\}_{i=1}^{n}$ by matching collectively the measurements $\{d_k\}_{k=1}^{N}$ to the model predictions $\{M_s(A_k,\omega_k)\}_{k=1}^{N}$ via the least-squares optimization. In particular, we formulate the following optimization problem

$$\min_{C} \frac{1}{2} \parallel HC - d \parallel_2^2 \quad (10)$$

where

$$H = \begin{bmatrix} h_1(A_1,\omega_1) & \cdots & h_n(A_1,\omega_1) \\ h_1(A_2,\omega_2) & \cdots & h_n(A_2,\omega_2) \\ \cdots & & \cdots \\ h_1(A_N,\omega_N) & \cdots & h_n(A_N,\omega_N) \end{bmatrix}, C = \begin{bmatrix} c_1 \\ c_2 \\ \cdots \\ c_n \end{bmatrix}, \text{ and}$$

$$d = \begin{bmatrix} d_1(A_1,\omega_1) \\ d_2(A_2,\omega_2) \\ \cdots \\ d_N(A_N,\omega_N) \end{bmatrix}$$

The above least-square optimization problem can be readily solved. In this work, the command *lsqnonlin* in Matlab is used to solve (10).

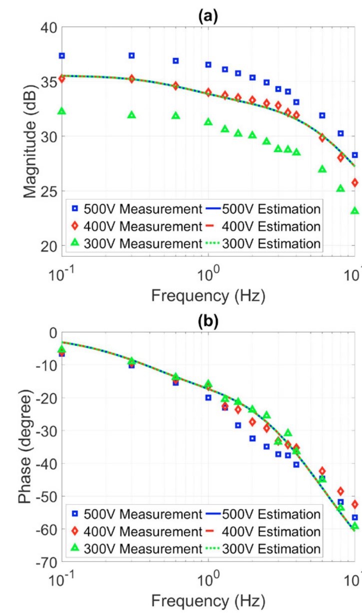

Fig. 6. Comparison of measured (a) magnitude and (b) phase frequency responses with model-predicted frequency responses under different input amplitudes ($n = 1$).

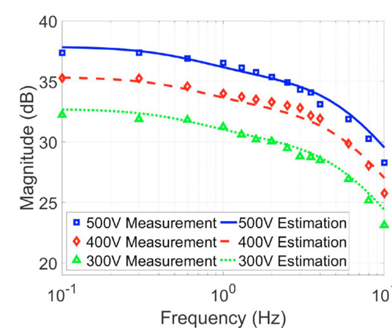

Fig. 7. Comparison of measured magnitude frequency responses with model-predicted frequency responses under different input amplitudes ($n = 2$).

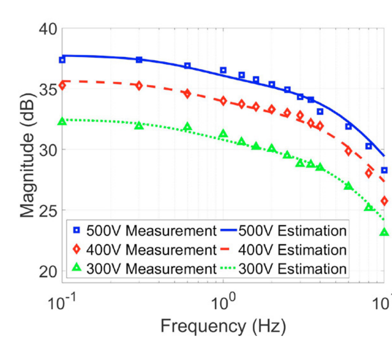

Fig. 8. Comparison of measured magnitude frequency responses with model-predicted frequency responses under different input amplitudes ($n = 3$).

4. EXPERIMENTAL RESULTS

We evaluate the proposed modeling and parameter identification approach in Section 3 with experimental data collected on the setup shown in Fig. 3. Sinusoidal voltage inputs of three different amplitudes (300 V, 400 V, and 500 V), with a fixed DC bias of 500 V, are applied to a PVC gel actuator. For each amplitude, inputs of 14 different frequencies, from 0.1 Hz to 10 Hz, are applied for 50 seconds. The corresponding actuator displacement is captured via the laser sensor for each amplitude and frequency used. Using fast Fourier transform, we obtain the amplitude and the phase of the displacement at the input frequency, with which we further compute the overall system gain and phase shift for the given input amplitude and frequency.

The measured (empirical) frequency response (both magnitude and phase responses) at the lowest input amplitude, 300 V, is used to identify the LTI component, $G(s)$. As shown in Fig. 5, the empirical response can be captured with a second-order system, identified with the Matlab function *tfest*:

$$G(s) = \frac{1200s + 8750}{s^2 + 44.49s + 212}$$

The nonlinear function f is identified with different degrees for the polynomial, $n = 1, 2, 3$, and the corresponding identified parameters c_i are listed in Table 2.

Table 2. Calculated polynomial parameters.

Polynomial	c_1	c_2	c_3
$n = 1$	1.4332	-	-
$n = 2$	0.5642	1.3954×10^{-5}	-
$n = 3$	0.2554	2.5146×10^{-5}	-1.9649×10^{-11}

When $n = 1$, the nonlinear function f degenerates to a linear relationship, and the resulting model is independent of the input amplitude and fails to capture the input-dependent dynamic behavior (Fig. 6). The model for $n = 2$ and $n = 3$ polynomial cases are shown in Fig. 7 and Fig. 8, respectively. Both models are able to capture the input-dependent dynamic behavior adequately; the model with $n = 3$ shows modest improvement over the model with $n = 2$, with the residual error norm in the least-squares estimation, Eq. (10), being 30% smaller than the case with $n = 2$. The phase plots for all models coincide with the one for $G(s)$ and are thus omitted for the cases of $n = 2$ and $n = 3$, and we note that the errors between the model-predicted phase and experimental measurements under different input amplitudes are small in general.

The dynamic models are further validated with the measured time-domain data from experiment. Figs. 9, 10, 11 show the comparison of the measured actuator displacement and the model-predicted displacement at two different frequencies (0.1 Hz and 10 Hz) for different polynomial degrees ($n = 1, 2, 3$), for input amplitudes of 300 V, 400 V, and 500 V, respectively. These results show that, when $n = 1$ (linear model), the model is only able to predict well the displacement output under an input amplitude of 400 V, while the models with $n = 2$ and $n = 3$ are able to capture well the displacement at all three levels of input amplitude. With the negligible improvement from $n = 2$ to

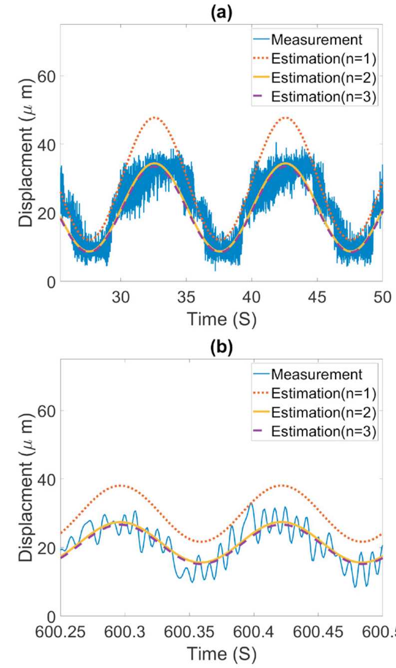

Fig. 9. Model-predicted output (for $n = 1, 2, 3$) versus measured output for PVC gel actuator with input amplitude of 300V: (a) 0.1 Hz, and (b) 10 Hz.

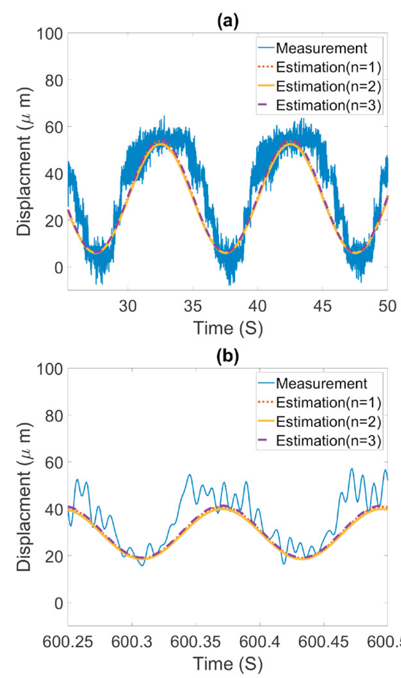

Fig. 10. Model-predicted output (for $n = 1, 2, 3$) versus measured output for PVC gel actuator with input amplitude of 400V: (a) 0.1 Hz, and (b) 10 Hz.

$n = 3$, it is determined that a model with $n = 2$ would be optimal in striking the trade-off between model accuracy and complexity.

5. CONCLUSION

In this paper, we have developed a framework for identifying a nonlinear dynamic model of a PVC gel actuator.

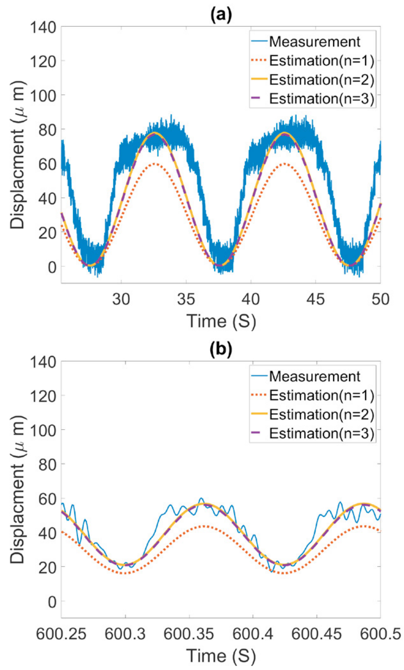

Fig. 11. Model-predicted output (for $n = 1, 2, 3$) versus measured output for PVC gel actuator with input amplitude of 500V: (a) 0.1 Hz, and (b) 10 Hz.

The approach adopts a Hammerstein model structure and uses the describing function methodology to identify the nonlinear element of the model. It was shown that the proposed model, with a polynomial consisting of linear and cubic terms preceding an LTI system, was able to capture the actuator's measured responses under different input amplitudes. The developed model is inherently control-oriented, and our future work will focus on the design of feedback controllers based on the developed model.

REFERENCES

Ali, M., Ueki, T., Tsurumi, D., and Hirai, T. (2011). Influence of plasticizer content on the transition of electromechanical behavior of PVC gel actuator. *Langmuir*, 27(12), 7902–7908.

Asaka, K. and Hashimoto, M. (2018). Electrical properties and electromechanical modeling of plasticized PVC gel actuators. *Sensors and Actuators B: Chemical*, 273, 1246–1256.

Asaka, K. and Hashimoto, M. (2020). Electromechanical modeling of plasticized PVC gel actuators and the improvement in their performances with the additions of ionic liquids. In *Electroactive Polymer Actuators and Devices (EAPAD) XXII*, volume 11375, 1137511 (13pp). International Society for Optics and Photonics.

Choi, H.R., Jung, K., Ryew, S., Nam, J.D., Jeon, J., Koo, J.C., and Tanie, K. (2005). Biomimetic soft actuator: design, modeling, control, and applications. *IEEE/ASME Transactions on Mechatronics*, 10(5), 581–593.

Frank, Z., Olsen, Z., Hwang, T., and Kim, K.J. (2019). Modelling and experimental study for PVC gel actuators. In *Dynamic Systems and Control Conference*, volume 59162, V003T20A007 (6pp). American Society of Mechanical Engineers.

Furuse, A. and Hashimoto, M. (2017). Development of novel textile and yarn actuators using plasticized PVC gel. In *Electroactive Polymer Actuators and Devices (EAPAD) 2017*, volume 10163, 1016327 (11pp). International Society for Optics and Photonics.

Hirai, T., Ali, M., Ogiwara, T., Tsurumi, D., Yamamoto, K., Ueki, T., Xia, H., and Hashimoto, M. (2013). Characteristic electrical actuation of plasticized poly (vinyl chloride): Various electrical functions in relation with the dielectric plasticizers. In *Advances in Science and Technology*, volume 79, 1–6. Trans Tech Publ.

Hirai, T., Ogiwara, T., Fujii, K., Ueki, T., Kinoshita, K., and Takasaki, M. (2009). Electrically active artificial pupil showing amoeba-like pseudopodial deformation. *Advanced Materials*, 21(28), 2886–2888.

Hwang, T., Frank, Z., Neubauer, J., and Kim, K.J. (2019). High-performance polyvinyl chloride gel artificial muscle actuator with graphene oxide and plasticizer. *Scientific Reports*, 9(1), 1–9.

Li, Y., Guo, M., and Li, Y. (2019). Recent advances in plasticized PVC gels for soft actuators and devices: a review. *Journal of Materials Chemistry C*, 7(42), 12991–13009.

Li, Y. and Hashimoto, M. (2015). PVC gel based artificial muscles: Characterizations and actuation modular constructions. *Sensors and Actuators A: Physical*, 233, 246–258.

Li, Y. and Hashimoto, M. (2016). Design and prototyping of a novel lightweight walking assist wear using PVC gel soft actuators. *Sensors and Actuators A: Physical*, 239, 26–44.

Li, Y., Maeda, Y., and Hashimoto, M. (2015). Lightweight, soft variable stiffness gel spats for walking assistance. *International Journal of Advanced Robotic Systems*, 12(12), 175 (7pp).

Park, W.H., Shin, E.J., and Kim, S.Y. (2017). Enhanced design of a soft thin-film vibrotactile actuator based on pvc gel. *Applied Sciences*, 7(10), 972 (12pp).

Park, W.H., Shin, E.J., Yoo, Y., Choi, S., and Kim, S.Y. (2019). Soft haptic actuator based on knitted pvc gel fabric. *IEEE Transactions on Industrial Electronics*, 67(1), 677–685.

Sharif, M.A., Lei, H., Al-Rubaiai, M.K., and Tan, X. (2018). Ionic polymer-metal composite torsional sensor: physics-based modeling and experimental validation. *Smart Materials and Structures*, 27(7), 075039 (9 pp).

Shibagaki, M., Ogawa, N., and Hashimoto, M. (2010). Modeling of a contraction type PVC gel actuator. In *2010 IEEE International Conference on Robotics and Biomimetics*, 1434–1439. IEEE.

Slotine, J.J.E., Li, W., et al. (1991). *Applied Nonlinear Control*, volume 199. Prentice hall Englewood Cliffs, NJ.

Xia, H. and Hirai, T. (2009). Space charge distribution and mechanical properties in plasticized PVC actuators. In *2009 International Conference on Mechatronics and Automation*, 164–169. IEEE.